Indian Journal of Pure & Applied Physics
Vol. 60, June 2022, pp. 529-538

Preparation and Investigation of Transparent Conducting Aluminium-doped Zinc Oxide Films Prepared by Sol-gel Method for Sensor Application

Prabhjot Singh[a], Sukhmander Singh[b*], Jasmeet Kaur[a], Sonia Yogi[c] & Bhavna Vidhani[c]

[a]Department of Physics, Guru Nanak Dev University, Amritsar, Punjab-143 005, India.

[b]Plasma Waves and Electric Propulsion Laboratory, Department of Physics, Central University of Rajasthan, Ajmer, Kishangarh- 305 817, India

[c]Department of Physics & Electronics, Hansraj College, University of Delhi, Delhi-110 007, India

Received 20 February 2022; accepted 9 May 2022

Aluminium doped Zinc Oxide (AZO) thin films were prepared through chemical route using sol gel method at different annealing temperatures with three different concentrations of Al. It has been observed that on increasing in the annealing temperature, the crystallinity of the films improved. The XRD patters confirms the polycrystalline nature of the samples and found that increasing annealing temperature, increases the crystallinity of the films. The UV-vis spectroscopy analysis shows that, the band-gap decreases in all three concentration of Al ions in ZnO with temperature. The conductivity and the grain size increases with temperature. The band gap corresponding to the absorption decreases with increased annealing temperature.

Keywords: X-Ray spectra; Optical properties; Electrical properties; Photolumniscence

1 Introduction

Semiconductor nanomaterials have a lot of applications due to their size dependent structural, optical and electrical properties. Zinc oxide (ZnO) nanostructure is one of most important semiconductor material due to large number of electronic applications. Zinc oxide used in a lot of electronic applications such as gas sensors[1,2], Photocatalytic performances, Light emitting diodes (LEDs), solar cells, Schottky diode, bacterial sensor, UV photodetector, photoconductor sensors and nonlinear optical devices.

Transition metal oxides are low dimensional nanostructured materials with the unique physical properties (easily available, good transparency, high electronmobility, strong room-temperature luminescence, etc.) and chemical properties. Zinc oxide nanostructure are one of the most vital semiconductor materials due to large variety of electronic applications. Hexagonal wurtzite structured Zinc oxide nanomaterials are well-known n-type (II-IV) semiconductors and exhibits interesting properties. It is a wide band-gap semiconductor with a direct band-gap of 3.2–3.36 eV and an exciton binding energy of 60 meV at ambient temperature[1,2]. ZnO is Wurtzite structured and ideal to incorporate with Aluminium. It falls in the category of transparent conductive oxides (TCOs) collectively with tin oxide (TO) and indium tin oxide (ITO)[5].

Various chemical and physical technique have been used to synthesize zinc oxide nanostructures along with sol-gel method[1-9], RF magnetron sputtering[10-15], chemical method[16-20], spray pyrolysis technique[21,22], hydrothermal method[23], Solid state reaction technique[24], Co-precipitation method[25], Silvaco TCAD Tool[26], SILAR method[27], atmospheric pressure plasma deposition process[28] and Melt quench technique[29].

For semiconductors such as ZnO, doping with transition metal elements is a beneficial tool to enhance its optical, electrical, mechanical and magnetic properties for the optoelectronic devices fabrication. Various doping elements such as Aluminium, Cerium, Gallium, Gadolinium, Copper, Iodine, Manganese, Magnesium, and Samarium *etc*., have been studied worldwide by a lot of researchers to investigate the physical, chemical, mechanical[14], electrical and magnetic[24] characteristics of the zinc oxide nanomaterials. Al_{3+} is the most widely used dopant due to small ionic radius and low cost.

Aluminium doped ZnO (AZO) film sensor show excellent NO_2[1] and SO_2[2] gas sensing characterstics.

*Corresponding author: (E-mail: sukhmandersingh@curaj.ac.in)

Oluwaseun *et al*.[3] prepared the ZnO and AZO thin films on the glass slides and found that optical band gap of AZO thin films decreases with increasing doping concentration. The thicknesses of the thin films increases with increased doping concentration increases. ZnO nanoparticles shows the antifungal activity. Bhargav *et al*. synthesized the Al and Cu doped ZnO nanoparticles and revealed that the doped ZnO nanostructures has better resistance against the growth of the fungus[4]. Norhidayah *et al*.[5] studied the electrical and optical properties of Gd doped ZnO thin films with different concentration. Their results shows that, the doped films has higher transmittance (~95 % in the visible region). The electrical measurement studies shows that the resistance decreases with higher Gd concentration. Islam *et al*.[6] fabricated the AZO thin films, which exhibit better photo catalysis efficiency than ZnO. The UV-Vis analysis shows that the doping leads to narrowing the band gap. The X-rays diffraction showed the polycrystalline nature of thin films. Mitra *et al*.[7] synthesized Facile AZO polyaniline hybrids for stronger visible-mild photo-degradation organic-inorganic hetero-structures. The photo degradation efficiency enhanced due to charge separation. Sandeep *et al*.[8] synthesized AZO films prepared by sol-gel spin coating technique, which is used as blue phosphors that generates white light. The enhanced blue emission the luminous efficiency (22.8%) increased considerably in AZO thin film in contrast to the ZnO film (10.8%). Serrao and Dharmaprakash synthesized transparent conductive gallium-doped ZnO films with different thickness by sol–gel spin coating technique and studied electrical, optical and structural properties[9].

Vasile *et al*. prepared the transparent Indium-doped zinc oxide and aluminium-doped zinc oxide thin films by radio-frequency magnetron sputtering on glass substrates and analysed the influence of sputtering power on the properties. The grazing incidence X-ray diffraction revealed the AZO thin films has wurtzite structure of zinc oxide while the IZO found in amorphous phase. The atomic force microscopy showed the uniform and smooth surfaces for all prepared structures[10]. Arumugam *et al*.[11] used 13.56 MHz radio-frequency magnetron sputtering system to deposit AZO thin film on glass. The Hall measurement revealed its n- type nature and the resistivity found to decrease with increase in sputter time.

Aitdads *et al*.[12] fabricated mixed halideperovskites thin films to produce the aluminum-doped Zinc oxide thin film through RF sputtering on indium-tin-oxide substrates. They also constructed a solar cell and the optical band gap of perovskite thin films was found 1.85eV. Kang *et al*.[13] fabricated Ga-Mg co-doped ZnO films on glass substrates by radiofrequency magnetron sputtering and found that growth temperature affects the mechanical, optoelectronic and structural properties of Ga-Mg co-doped ZnO films. Pat *et al*.[14] obtained nanomechanical property of ZnO and AZO thin films using RF sputtering technique. The crystallite size of thin films was measured around 20 nm (AZO) and 35nm (ZnO). The measurement shows that its roughness values 3.15 nm, hardness 11 GPa and Young's modulus 95 GPa. In case of ZnO that its roughness values 5.15 nm, hardness 7 GPa and Young's modulus 155 GPa. A radio-frequency magnetron sputtered was used to create AZO thin films on glass by Tseng[15]. As the annealing period is raised from 40 seconds to 1800 seconds, grain sizes fall from 13 nm to 9.3 nm. Ahmed *et al*.[16] prepared the Sm doped ZnO nanorods with chemical bath deposition method and observed the Schottky barrier height for pure and Sm doped ZnO nanorods 0.55 eV and 0.72 eV respectively. The growth rate of the nanorods found to suppressed and the UV emission is slightly red shifted by Sm doping. Bomila *et al*.[17] synthesized Ce doped ZnO nanoparticles to investigate its antibacterial, optical and structural properties. The optical band gap value (ZnO) decreases and visible emission increseas with Ce doping. Hitkari *et al*.[18] used chemical method to synthesiz ZnO and ZnO–ZnS nanocomposite materials and revelaed that optical band gap decreases with doping. The ZnS- ZnO composite film show higher dye degradation efficiency than pure ZnO. Kumar *et al*. used chemical bath deposition technique to synthesize AZO thin films and to investigate the doping effect on its physical and optical properties. It is found that , the transmittance is reduced with higher doping and the optical transmittance is found 87% in the visible region[19]. Majumder *et al*.[20] synthesized AZO film with 0.30 Ohm-cm resistivity. It is observed that doping beyond 4% enhance the resistivity of the films, since segregation of Al as oxide resulting electrons scattering. Ibraheam *et al*.[21] investigated UV Photodetector of Al:ZnO nanostructure and observed shift in energy band due to higher doping. Makuku *et al*.[22] investigated properties of Aluminum and gallium co-doped ZnO thin films and observed that The electrical

conductivity of ZnO thin films was increased by Co-doping.. Chakraborty *et al*.[23] studied Al and Cu co-doped ZnO nanorods which shows remarkable enhancement in current density. Arora *et al*.[24] synthesized Sm dopped ZnO thin films by a solid state reaction method and observed that dopped films shows higher ferromagnetism at room temperature.

Belkhaoui *et al*.[25] studied the improvement of crystalline quality, conductivity and optical property of Mn doped ZnO produced by co-precipitation process. Variation of thickness of AZO thin film improves the performance of photoconductor sensor and the doping lower the AC conductivity due to the enhancement of defects amount but higher the average crystallite size growths found[26]. Abdullah *et al*. employed Silvaco TCAD tool to fabricate the AZO photoconding thin films and doping improved the electrical features of the device[27]. Edison *et al*.[27] synthesized AZO thin films to investigate the 3rd order non linear optical parameters of films using z-scan technique to explore the application in non linear device. The optical transmittance found to decreases with

dipping cycles and its value found to 87% (visible region) with band gap 3.23 eV. Favaro *et al*.[28] employed atmospheric pressure plasma coating technique to synthesize homogenous oxide phase of AZO thin films and its conducitivity improved with doping. Singh *et al*.[29] analyzed the optical and structural properties of Al_2O_3–PbO–B_2O_3 doped with CeO_2 and ZnO glasses. It has been revealed that optical band gap decreases while the refractive index, molar refraction and density increases with doping. Tappura *et al*. deposited AZO thin films on flexible substrates for the applications of large-area thermoelectric generator and evaluated its performance near the room temperature[30]. AZO thin film based gas sensors are prepared by Chaitra *et al.*to detect the low concentration of Sulphur dioxide and explored that sensing performance improves with doping of aluminium concentration. Crystal size found to reduced and wrinkle strcture was observed during characterizations[31]. Nizamani *et al*. prepared transparent conductive oxides D shaped optical fibre with AZO thin films coating which worked as a saturable absorber and enhanced the nonlinearty effects[32]. Farsi *et al*. employed microwave method to synthesize a quasi-aligned AZO nanorods at 1% and 5% concentrations[33]. Villegas *et al*. used pray-pyrolysis technique to synthesize the AZO transparent conducting films and evalauted that microstructures properties improves with doping amounts. The resistance of the film reduced with doping and opposite effects were observed with extra doping[34].Tönbül *et al*. used ultrasonic spray pyrolysis method to prepare the AZO thin films of 750 nm thickness, which posses 83% transmittance in the visible region and good thermal resistance value[35]. Jyothish and Jacob synthesized aluminium-doped zinc ferrite nanoparticles and studied the anti cancer, morphological, thermal and structural properties. The micro strain values and band gap are decreases with increasing annealing temperatures. The emission scanning electron microscopy revealed the particle size of hundered nanometer[36].

The Spin coating is easy and fast method to generate homogeneous and thin films out of solution. The centrifugal force of rotating high speed spin-coater base is utilized to apply uniform thin films to flat substrates. One of the major lead of the spin coating technique is that the thicknesses of film may easily change by switching to a different viscosity, or changing the spin speed to get variable outcomes[37,38]. The main disadvantage of spin coating processes is that it utilizes only 2-5 % of the material is distributed over onto the substrate, while the remaining 95-98 % is thrown into the coating bowl and disposed. So the disposal of solution as low material efficiency and the repeated coating cause accumulation of more solution at the edges and when the beaded fluid dries, the remaining resist flows over the step and dries and increasing the edge beading effect contributes as major disadvantages.

The aim of this article to investigate the structural, optical and electrical properties of AZO thin films prepare by sol gel process between doping concentration and annealing temperature parameters[39-46]. This article is organized in the following way: Material methods and experimentation section 2 describes the film preparation by using sol-gel spin coating technique. The film characterization methods are given in section 3. The results and the discussion section elucidate the deposition process, which has been finalized by repeatedly experimenting on selecting different parameters like rotating speed, drying temperature, deposition rate and number of coatings to get effectual outcomes. Further, in result and discussion section, a report of the optical, electrical and structural properties of the aluminium doped ZnO films has been given in section 3. Finally, Sec. 4 is devoted to conclusions.

2 Experimental Details

In order to prepare AZO solutions, the zinc acetate dehydrate was dissolved in 2-methoxyethanol (MOE) and aluminum chloride hexa hydrated served as dopant sources (in AZO). The solution concentration was 0.5 mol/L with Al doping concentrations (molar) 4%, 8% and 12% respectively. Then the prepared solution is set in steering with magnetic steerer for 1 h. The spin coating unit was used for the uniform deposition of AZO films. the adjusted parameters of the spin coating unit are given in Table 1.

After setting parameters, the thin film deposition of solution AZO solutions, process involves placing pre-cleaned square (25 X 25 mm^2) quartz substrate, 1.5 mm thick on the chunk of top plate assembly of the spin coating unit. Then, 5-6 droplets of the solution were poured on the glass substrate using a dropper. The substrate was accelerated up to its final desired rotation speed following stage 1 as given in the Table 1. The films were heated at 300 ^{o}C for 10 minutes and the process was repeated for 15 times with each sample solution. After this, three different film samples of same Al doping concentration were annealed in a furnace at 500 °C, 700 °C and 900 °C for 5 hours.

The structural analysis of the films was done using X-ray diffraction (XRD) Bruker D8 focus was carried out using filtered Cu Kα radiation operated at voltage 40 kV and current 30 mA. X-ray diffract gram has been recorded in the range 25^{o}-60^{o} (2θ) at a scanning speed of 2^{o} per minute. All structural measurements were taken at room temperature. The UV-Perkin Elmer λ-35 spectrophotometer is used to obtain the absorbance spectra of the samples at room temperature in the wavelength ranging from 200 nm to 1100 nm. The band gap of the films was calculated by Bardeen relation,

$$\alpha h\nu = B(h\nu - E_g)^n \quad \ldots (1)$$

The fluorescence LS 45 is used to obtain the photoluminescence and to measure the PL emission intensity over a range of wavelengths. The electrical properties were studied buy using the two-line probe method, two lines of silver glue drawn on the sample and spaced by L (as shown in figure arrangement), on thin film. The voltage of the *Keithley* 6517-A instrument as source of +5 V. For each scan, 100 resistivity points were recorded with the falling temperature from 140 ^{o}C to 40 ^{o}C.

Table 1 — Details of parameters selected

Spin	Rpm	Time(sec)
Stage	2500	30

3 Results and discussions

3.1 Structural characterization

The X-ray diffraction pattern of AZO thin film with composition $Zn_{1-x}Al_xO$ solutions films shows the single prominent peak at 2θ = 34.52^{o}. The corresponding indices (002), confirms the presence of wurtzite phase and the dopant Al occupied the place of Zn in wurtzite structure and the zinc oxide film doped with aluminium shows along the (0 0 2) plane as a preferred orientation. It shows that the small amount of doping of aluminium in the zinc oxide films promotes as *c*-axis orientation[18]. Although the corresponding peaks of indices (100) and (101) are obtained at 2θ = 32.92^{o} (100) and 2θ = 36.45^{o} (101) intensity respectively.

All the samples show peaks at 31.25^{o}, 34.52^{o}, 36.45^{o}, 47.85^{o} and 57.5^{o} which are corresponds to the hexagonal wurtzite structure of ZnO crystal lattice. It is clear that (002) peak is dominant in all the samples with preferred orientation along c-axis. No peak corresponding to Al ions were observed, which indicate the absence of any secondary phase in thin film samples. Whilst, the structure remains in single phase till 12% of Al doping concentration. In fact, the increase in peak intensities shows more stability of the film samples at higher concentrations.

XRD patterns of the deposited films has been shown in Figs. 1-4 and it was observed that higher annealing temperature, improves the crystallinity of the samples. This is due to the stress released between the planes of the lattice structure to release the excess energy. This leads to the unidirectional orientation of the planes towards the preferred c-axis. It is also noticed that with increase in temperature, the dopant do not show any of its indegenous peak, which

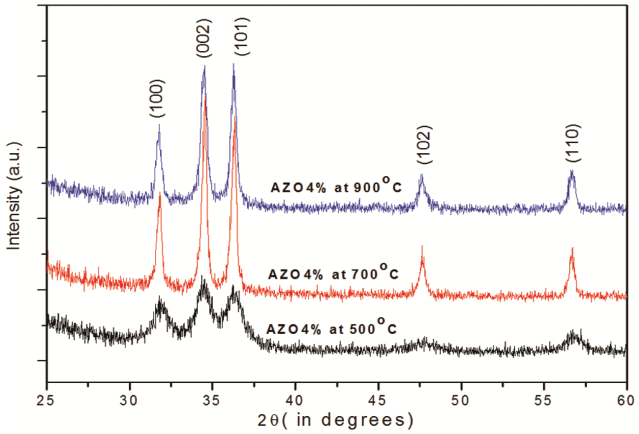

Fig. 1 — X-ray diffraction of Al-doped ZnO 4% thin films at 500 °C,700 °C and 900 °C annealing temperature.

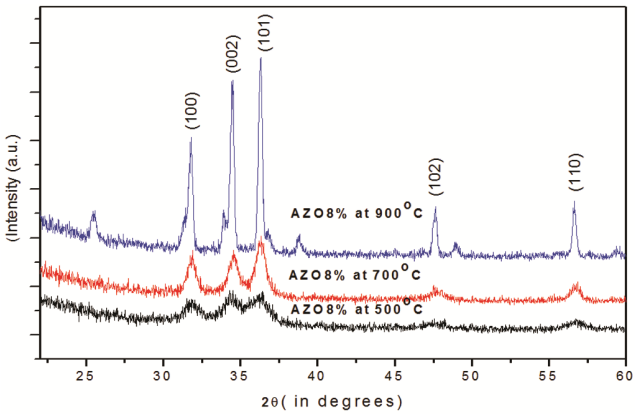

Fig. 2 — X-ray diffraction of Al-doped ZnO 8% thinfilms at 500 °C,700 °C and 900 °C annealing temperature.

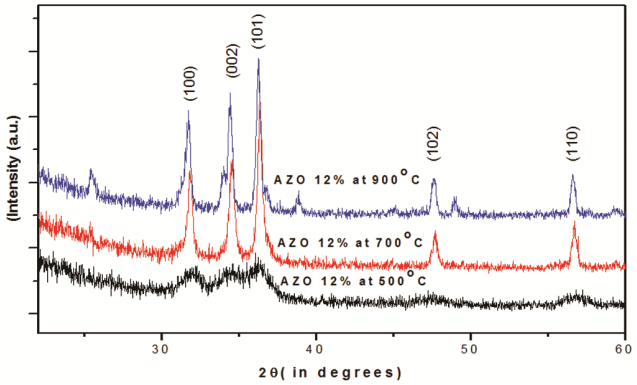

Fig. 3 — X-ray diffraction of AZO12% thin films at 500 °C, 700 °C and 900 °C annealing temperature.

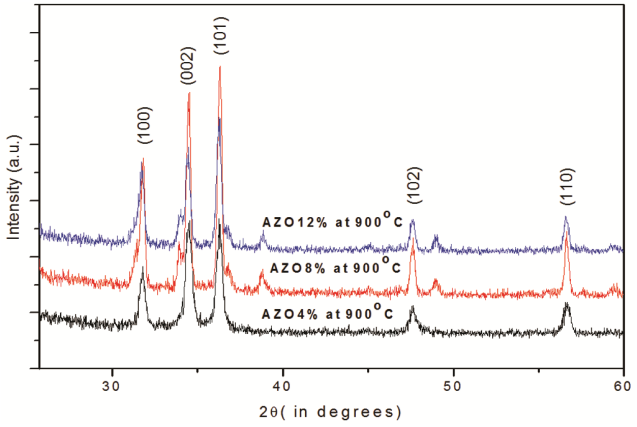

Fig. 4 — Comparative X-ray diffraction with different concentration of AZO thinfilms at 900 °C annealing temperature.

reveals its incorporation in the wurtzite lattice of ZnO thin films. Therefore, the film crystallinity remains unaffected with the dopant concentration and no preferential deposition takes place along any axis [47]. At low concentrations of Al^{3+} ions, the crystallize size does not affected as the defects being neutralized, but

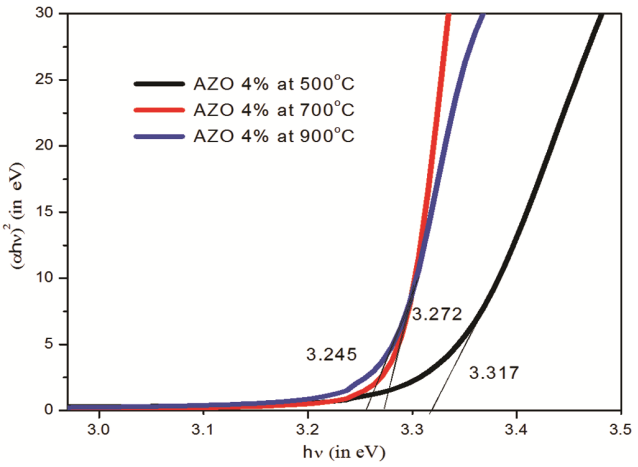

Fig. 5 — Plot of $(\alpha h\nu)^2$ *vs* energy (hν) at 4% Al doping at annealing temperature 500 °C, 700 °C and 900 °C.

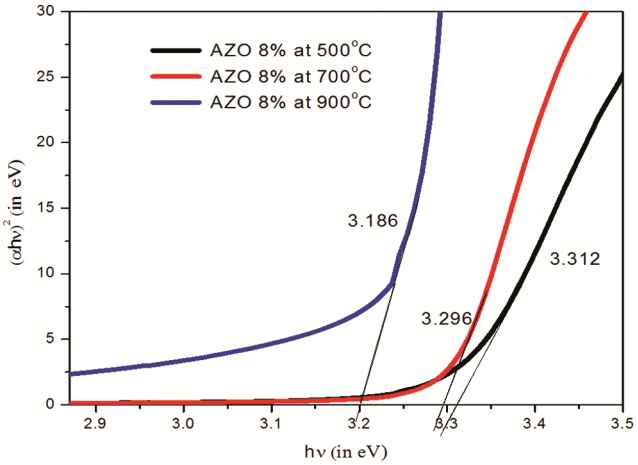

Fig. 6 — Plot of $(\alpha h\nu)^2$ *vs* energy (hν) at 8% Al doping at annealing temperature 500 °C, 700 °C and 900 °C.

the strain and size became dependent on thickness as on increasing the concentration of aluminium. Volume contraction of the lattice being indicated by the increases in density on increases in the concentration of aluminium, which is responsible for the low peak intensity of the AZO thinfilm with composition $Zn_{0.88}Al_{0.12}O$ further supported by a axial ratio (c/a) change of the film.

3.2 UV-VIS Spectroscopy

The transmission optical spectra using UV Visible spectroscopy has been shown in Figs 5-7 of $Zn_{1-x}Al_xO$ (x=0.04, 0.08 and 0.12) thin films with annealing temperature 500 °C, 700 °C and 900 °C. From optical absorption spectroscopy, the band gap variations of $Zn_{1-x}Al_xO$ thin film determined by using Tauc's plot between *hν* and $(\alpha h\nu)^2$, where α being the coefficient of absorption. For allowed direct transition relation

between band gap, E_g and α given by[19] and expressed as $\alpha h\nu \propto (h\nu - E_g)^{1/2}$. $Zn_{1-x}Al_xO$ (x = 0.04, 0.08 and 0.12) thin film, the UV spectra in Table 2 shows a decrease in the band gap for corresponding temperatures 500 °C, 700 °C and 900 °C.

UV-VIS spectroscopy analysis shows, that optical band gap decreases with increasing annealing temperature for the fixed value of Al doping of 12%. Since, the increased doping concentrations enhances the free electrons, which results in the reduced band gap of the films. The changes in the carrier concentration and shift of the band-gap can be explained by the Burstein-Moss shift[48-52]. It implies that the results of optical transmission spectra are also consistent with Al^{3+} ions doping, substitute Zn^{2+} ions in its wurtzite lattice structure. From the Fig. 8, it has also been observed that there is a slight decrease in the band gap with increase in concentration of AZO films. The observed result in the band shift is due to the increment in the free charge carries with an increases in doping concentrations of aluminium ions in zinc oxide thin films sample.

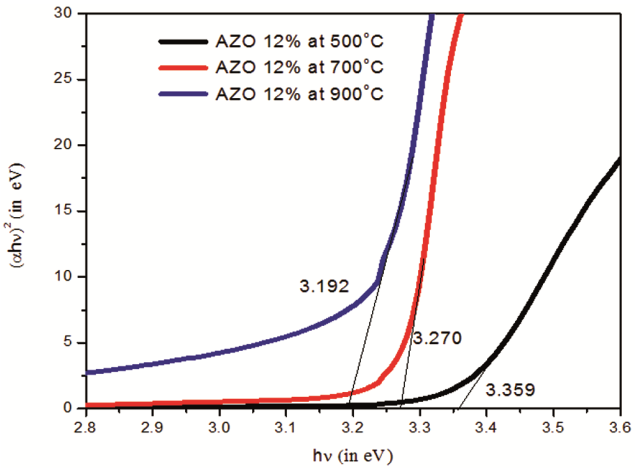

Fig. 7 — Plot of $(\alpha h\nu)^2$ *vs* energy (hν) at 12% Al doping at annealing temperature 500 °C, 700 °C and 900 °C.

3.3 UV-VIS transmittance spectra

UV-VIS transmittance spectra of AZO films are plotted between transmittance (%) and hν (eV) of 4 %, 8 % and 12 % concentration at 500 °C, 700 °C and 900 °C annealing temperatures in Figs. 9-11. The Fig. 12 shows the comparative analysis of UV-VIS transmittance spectra of AZO films with different

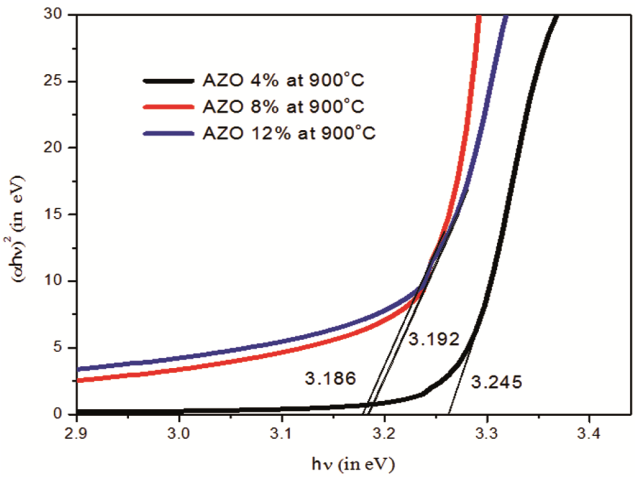

Fig. 8 — Comparative Plot of $(\alpha h\nu)^2$ *vs* energy (hν) with different concentration of AZO thin films at annealing temperatures 900 °C.

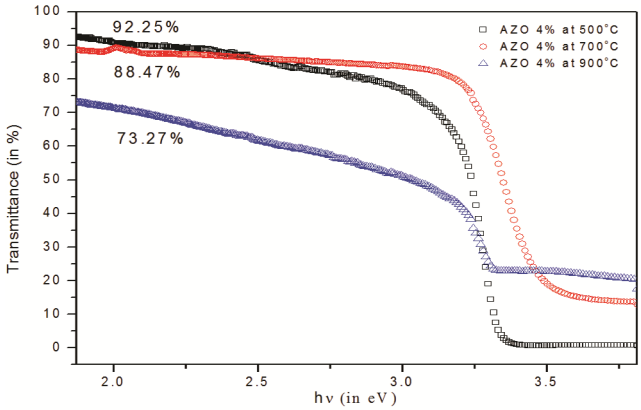

Fig. 9 — UV-VIS transmittance spectra of 4% AZO (Aluminium doped Zinc Oxide) films between transmittance (in%) and hν (nm) at 500 °C,700 °C and 900 °C annealing temperatutres.

Table 2 — Estimated bang gap energies as a function of annealing temperatures.

Doping Concentration (%)	Annealing Temperature (ºC)	Band Gap (eV)	Transmittance (%)
4	500	3.317±0.003	92.25
4	700	3.272±0.002	88.47
4	900	3.245±0.002	73.27
Doping Concentration (%)	Annealing Temperature (ºC)	Band Gap (eV)	Transmittance (%)
8	500	3.312±0.002	96.61
8	700	3.296±0.002	76.24
8	900	3.180±0.002	68.67
Doping Concentration (%)	Annealing Temperature (ºC)	Band Gap (eV)	Transmittance (%)
12	500	3.359±0.002	93.11
12	700	3.270±0.002	87.37
12	900	3.192±0.002	73.83

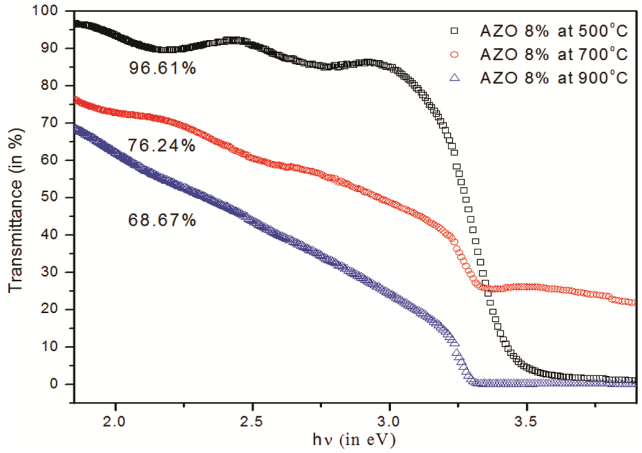

Fig. 10 — UV-VIS transmittance spectra of 8% AZO films between transmittance (in%) and hv (in eV) at 500 °C,700 °C and 900 °C annealing temperatutres.

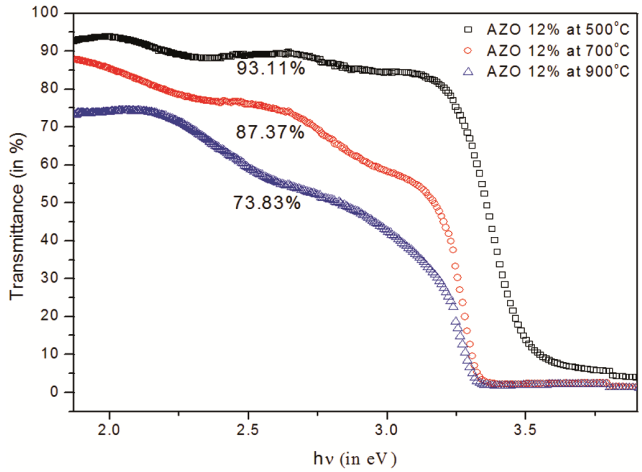

Fig. 11 — UV-VIS transmittance spectra of 12% AZO films between transmittance (in%) and hv(in eV) at 500 °C,700 °C and 900 °C annealing temperatutres.

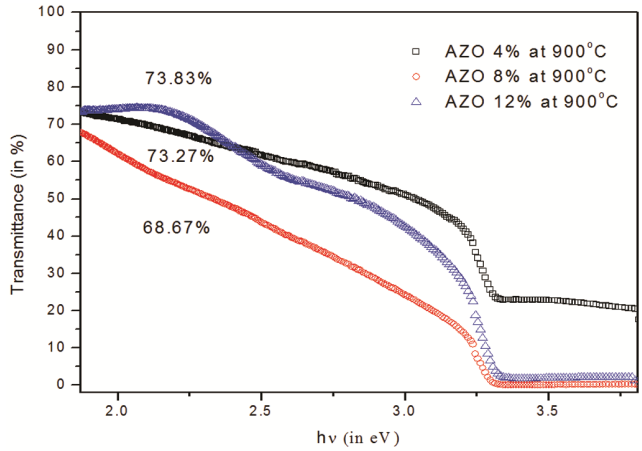

Fig. 12 — Comparative UV-VIS transmittance spectra of AZO films with different concentration between transmittance (in%) and hv(in eV) at 900 °C annealing temperatutres.

concentration between transmittance (in%) and hv (in eV) at 900 °C annealing temperatutres.The trend of lower transmittance with increase in annealing temparature and concentration are observed. This is due to the increase in some voids or defect centers, which caused the increase in light scattering and hence transmission decreases.

3.4 Photoluminescence

PL spectra of the samples prepared with different Al ion concentration were obtained with the excitation wavelength at 330 nm at room temperature. From the Figs. 13-16, it is clear, that all the sample shows narrow Full-Width at Half-Maximum (FWHM) with strong UV emission of the near band edge (around 384 nm) due to the annihilation of excitons. A broad peak is identified around at 490–530 nm, which refers

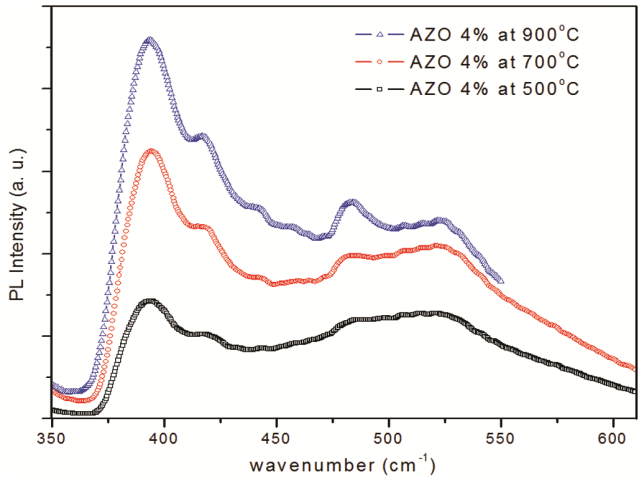

Fig. 13 — PL spectra of 4 % AZO films annealed at temperature 500 °C, 700°C and 900 °C

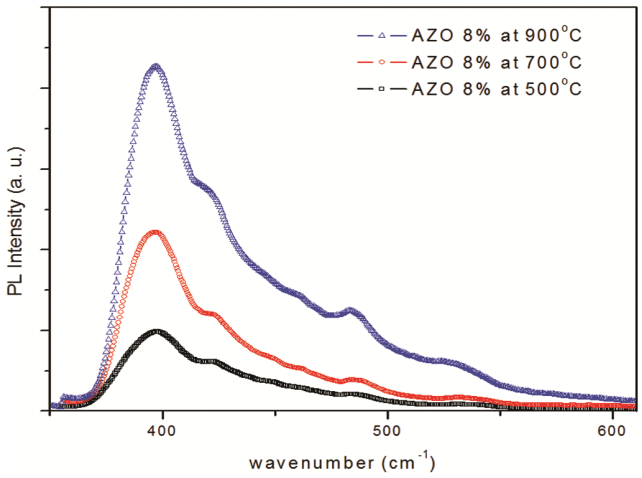

Fig. 14 — PL spectra of 8 % AZO films annealed at temperature 500 °C, 700 °C and 900 °C

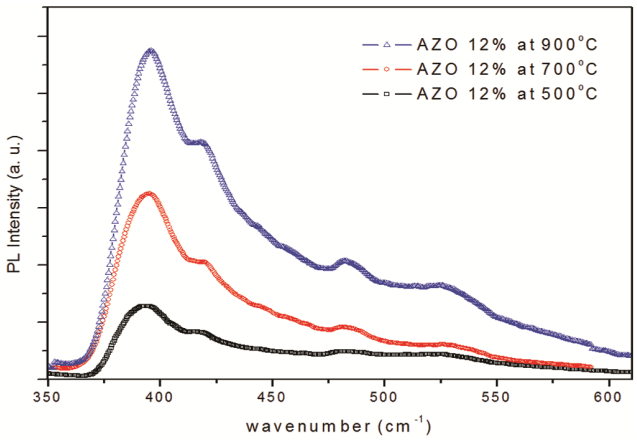

Fig. 15 — PL spectra of 12 % AZO films annealed at temperature 500 °C,700 °C and 900 °C

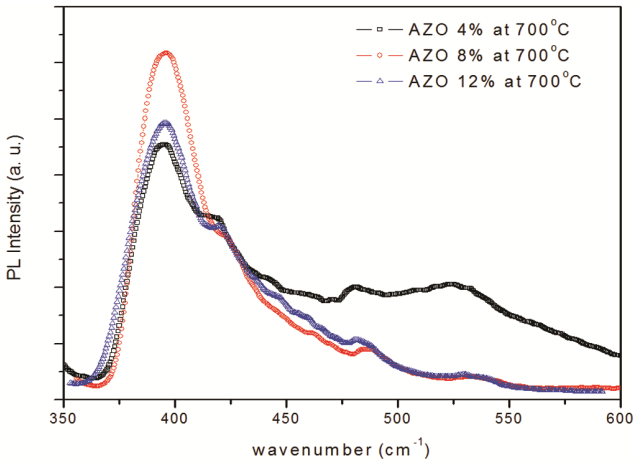

Fig. 16 — Comparative PL spectra of different concentration of AZO films annealed at temperatures 700°C.

to the green emission in all the samples. The intensity of peak at 384 nm increases with highr temperature. The increase in peak intensities might be due to the more stable incorporation of Al^{3+} ions with the increase in temperature of 4 %, 8 % and 12 % Al doped ZnO film samples. But it is found that peak intensity of the PL spectra depends on the Aluminium concentrations. Due to the electron-hole recombination, UV band-edge emissions of high strength is observed, when the concentration of Aluminium in the target is in the range of 0–8.0 wt.%. However, the UV band-edge emission peak intensity decrease rapidly, when concentration of aluminium in the target increases to 8.0–12.0 wt.% its due to the shift in Fermi level[42], which block some of lower levels as a result of high doping concentration at 12%. Fig. 16 shows comparative anaylsis of PL spectra obtained for the samples prepared at 700 ° C for different Al concentrations (0–12 wt.%).

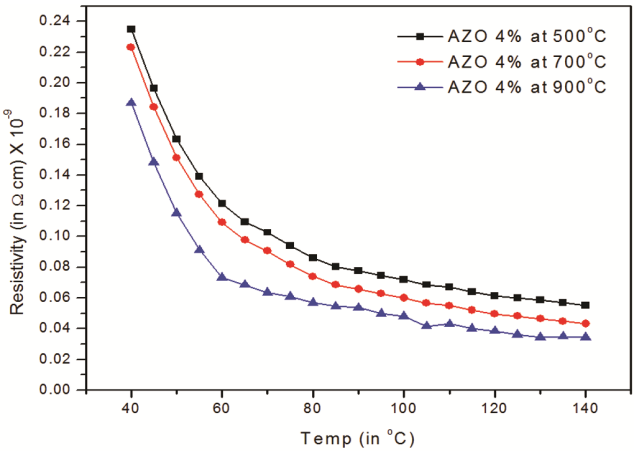

Fig. 17 — Resistivity *vs* temperature graphical representation of 4% AZO films annealed at temperature 500 °C, 700 °C and 900 °C.

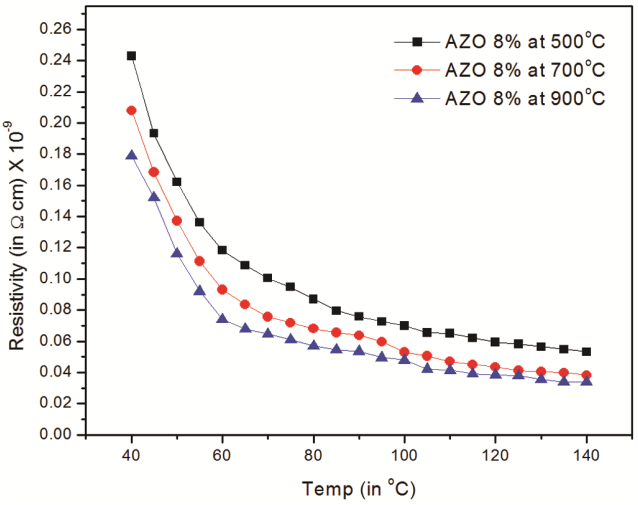

Fig. 18 — Resistivity *vs* temperature graphical representation of 8 % AZO films annealed at temperature 500 °C, 700 °C and 900 °C.

3.5 Electrical properties

The graphical representation of AZO thin films with doping concentrations (4%, 8% and 12%) using sol-gel spin coating method with annealed at different temperatures (500 °C, 700 °C and 900 °C) prepared by spin-coating technique has been shown in Figs 17-19. From the analysis it was observed that the resistivity of the films decreases with increase in temperature and Al doping concentration. This can be attributed to the increase in the grain size and available high concentration of free charge carriers in AZO films with the increasing annealing temperature. This reduces the grain boundary scattering and enhances the conductivity of thin film samples. The higher Al doping concentration provides excessive availability of free electron charge carrier for conduction than the lower Al ion concentration thin

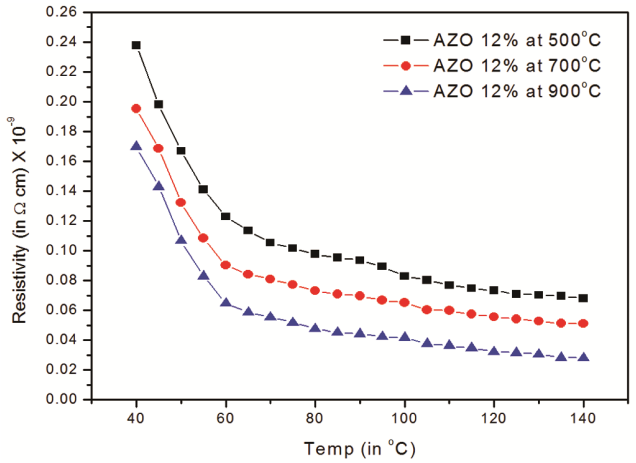

Fig. 19 — Resistivity *vs* temperature graphical representation of 12 % AZO films annealed at temperature 500 °C, 700 °C and 900 °C.

films annealed at the same temperature. The above trend observed in the electrical studies confirms the semi conducting behavior of the AZO thin films [53].

4 Conclusions

This study dedicated to investigate the structural, optical and electrical characteristics of post-annealing AZO thin films prepared by sol gel method. The XRD measurement of AZO thin films, discloses the hexagonal wurtzite structure of ZnO crystal lattice and the peak along (002) plane is dominant of all the samples with preferred orientation along c-axis. The calculated grain size increse as with increasing the annealing temperature. The results shows that the doping strongly alter the properties of the ZnO thin films. The studies also shows that the band-gap reduces with the concentration of Al ions in ZnO. The transmittance decreses with higher annealing temperatures and concentartion. Photoluminescence spectra shows the increase in peak intensities with the increase in temperature of film samples. The lower resistivity of the films was obtained with higher temperature.

References

1 Nimbalkar A R, Patil N B, Ganbavle V V, Mohite S V, Madhale K V & Patil M G, *J Alloys Compd*, 15 (2019) 466.

2 Chaitra U, Ali A V M, Viegas A E, Kekuda D & Rao K M, *Appl Surf Sci,* 496 (2019) 143724.

3 Oluwaseun A, Adetunji A J, Ibironke B D, Lydia A O & B I Taiwo, *J At Mol condens Nano phys,* 7 (2020) 25.

4 Bhargav P K, Murthy K S, Kaur K, Goyat M S, Pandey J K, Dubey S, Sharma S & Pant C, *Mater Res Innov*, 24 (2020) 385.

5 Cheani N, Sahdan M Z, Nayan N & Tawil S N M, *Adv Mater Res*, 1133 (2016) 424.

6 Islam M R, Rahman M, Farhad S F U & J Podder, *Surf Interfaces,* 16 (2019) 120.

7 Mitra M, Ghosh A, Mondal A, Kargupta K, Ganguly S & Banerjee D, *Appl Surf Sci*, 402 (2017) 418.

8 Sandeep K M, Bhat S & Dharmaprakash S M, *J Phys Chem Solids*, 104 (2017) 36.

9 Serrao F J & Dharmaprakash S M, *Mater Res Innov*, 20 (2016) 470.

10 Vasile N, Iftimie S, Acsente T, Locovei C, Călugăr AI, Radu A, Ion L, Antohe VA, Manica D, Toma O & Dinescu G, *Mater Res Express*, 6 (2020) 126447.

11 Arumugam S, Gopinath D & Lakshiminarayanan G, *Int J Adv Res Rev*, 2 (2017) 77.

12 Dads A H, Bouzit S, Nkhaili L, Elkissani A & Outzourhit A, *Sol Energy Mater Sol Cells*, 148 (2016) 30.

13 Kang H, Lu Z, Zhong Z & Gu J, *Mater Lett*, 215 (2018) 102.

14 Pat S, Mohammadigharehbagh R, €Ozen S, enay V S, Yudar H H & adanKorkmaz S, *Vacuum,* 141 (2017) 210.

15 Yang C R, Tseng S F & Chen Y T, *Appl Surf Sci*, 444 (2018) 578.

16 Ahmed M A M, Mwankemwa B S, Carleschi E, Doyle B P, Meyer W E & Nel J M, *Mater Sci Semicond Process*,79 (2018) 53.

17 Bomila R, Srinivasan S, Venkatesan A, Bharath B & Perinbam K, *Mater Res Innov*, 22 (2018) 379.

18 Hitkari G, Singh S & Pandey G, *Nano-Struct Nano-Objects*, 12 (2017) 1.

19 Kumar K D, Valanarasu S, Rosario S R, Ganesh V, Shkir M, Sreelatha C J & AlFaify S, *Solid State Sci*, 78 (2018) 58.

20 Majumder S B, Jain M, Dobal P S & Katiyar R S, *Mater Sci Eng B*, 103 (2003) 16.

21 Ibraheam A S, Rzaij J M, Fakhri M A & Abdulwahhab A W, *Mater Res Express*, 6 (2019) 055916.

22 Makuku O, Mbaiwa F & Sathiaraj T S, *Ceram Int*, 42 (2016) 14581.

23 Chakraborty M, Mahapatra P & Thangavel R, *Thin Solid Films*, 612 (2016) 49.

24 Arora D, Asokan K, Mahajan A, Kaur H & Singh D P, *R Soc Chem*, 6 (2016) 78122.

25 Belkhaoui C, Mzabi N & Smaoui H, *Mater Res Bull*, 111 (2019) 70.

26 Abdullah M, Jumidali M, Yuseri N Y & Yusoff S M, *J Phys Conf Ser*, 1535 (2020) 012010.

27 Edison D J, Nirmala W, Kumar K D, Valanarasu S, Ganesh V, Shkir M & AlFaify S, *Physica B Condens Matter*, 523 (2017) 31.

28 Favaro M, Zanazzi E, Patelli A, Carturan S, Ceccato R, Mulloni V, Bortolotti M & Quaranta A, *Thin Solid Films,* 708 (2020) 138118.

29 Singh G P, Kaur S, Kaur P & Singh D P, *Physica B*, 407 (2012) 1250.

30 Tappura K, Juntunen T, Jaakkola K, Ruoho M, Tittonen I, Ritasalo R & Pudas M, *Renewable Energy,* 147 (2020) 1292.

31 Chaitra U, Ali A M, Mahesha M G, Kompa A, Kekuda D & Rao K M, *Superlatt Microst*, 155 (2021) 106903.

32 Nizamani B, Jafry A A, Salam S, Fizza G, Soboh RS , Khudus M A, Hanafi E, Yasin M & Harun S W, *Laser Phys*, 31 (2021) 055101.

33 Al- Farsi B, Al- Marzouqi F, Al-Maashani M, Souier M T, Myint M T & Al-Abri M Z, *Mater Sci Eng B*, 264 (2021) 114977.

34 Villegas E A, Ramajo L A, Lere M E, Castro M S & Parra R, *Mater Sci Semicond Process*, 121 (2021) 105412.

35 Tönbül B, Can H A, Öztürk T & Akyıldız H, *Mater Sci Semicond Process*, 127 (2021) 105735.

36 Jyothish B & Jacob J, *J Alloys Compd*, 863 (2021) 158352.

37 Majumder S B, Jain M, Dobal P S, Katiyar R S, *Mater Sci Eng B*, 103 (2003)16.

38 Chopra K L, Major S & Pandya D K, *Thin Solid Films*, 102 (1983) 1.

39 Lee J H, Ko K H & Park B O, *J Cryst Growth*, 247 (2003) 119.

40 Lee J B, Lee H J, Seo S H & Park J S, *Thin Solid Films*, 398 (2001) 641.

41 Kumar S, Kim Y J, Koo B H, Sharma S K, Vargas J M, Knobel M, Gautam S, Chae K H, Kim Y K & Lee C G, *J Appl Phys*, 05 (2009) 520.

42 Liu, Yaodong, Lian & Jianshe, *Appl Surf Sci*, 253 (2007) 3727.

43 Silva, Rodrigo F, Zaniquelli, Maria E D, *Thin Solid Films*, 449 (2009) 86.

44 Lin J P & J M, *Appl Phys Lett*, 92 (2008) 134103.

45 Mridha S & Basak D, *J Phys D*, 40 (2007) 6902.

46 Nunes P, Fortunato E, Tonello P, Fernandes F B, Vilarinho P & Martins R, *Vacuum*, 64 (2002) 281.

47 Behera D & Acharya B S, *J Lumin*, 128 (2008) 1577.

48 Minami T, Miyata T & Ihara K *et al*., *Thin Solid Films*, 494 (2006) 47.

49 Minami T, Nanto H & Takata S, *Jpn J Appl Phys*, 24 (1985) L605.

50 Minami T, Suzuki S & Miyata T, *Thin Solid Films*, 398 (2001) 53.

51 Hamberg I, Granqvist C G, Berggren K F, Sernelius B E & Engstron L, *Phys Rev B*, 30 (1984) 3240.

52 Selnelius B E, Berggren K F, Zin Z C, I Hamberg & Granqvist C G, *Phys Rev B*, 37 (1988) 244.

53 Musat V, Teixeira B, Fortunato E & MonteiroR C C, *Thin Solid Films*, 502 (2006) 219.